Adsorption (2015) 21:125–133
DOI 10.1007/s10450-015-9655-y

Activated carbons prepared from peanut shell and sunflower seed shell for high CO_2 adsorption

Shubo Deng · Bingyin Hu · Tao Chen · Bin Wang · Jun Huang · Yujue Wang · Gang Yu

Received: 10 November 2014 / Revised: 4 January 2015 / Accepted: 12 January 2015 / Published online: 23 January 2015

Abstract Biomass wastes are considered as cost-effective and sustainable precursors to prepare activated carbons for CO_2 capture. In this study, two biomass-derived activated carbons were prepared using peanut shell and sunflower seed shell, and the optimal activated carbons were obtained at low KOH/carbon ratio of about 1. The peanut shell derived activated carbon (P-973-1.00) and sunflower seed shell derived activated carbon (S-973-1.25) exhibited CO_2 uptake of 1.54 and 1.46 mmol/g, respectively, at 298 K and 0.15 bar, among the activated carbons with the highest CO_2 adsorption. Although P-973-1.00 had much lower surface area and micropore volume than S-973-1.25, it possessed higher CO_2 uptake at 298 K and 0.15 bar due to the higher volume of micropores in the range of 0.3–0.44 nm. The calculated higher isosteric heat values at lower CO_2 uptake indicated the strong affinity of CO_2 in these micropores. The ordered micro-sized pores in the activated carbons were favorable for CO_2 diffusion into the porous materials and adsorption in the inner micropores. The activated carbons had moderate CO_2 selectivity over N_2 at 1 bar, but the selectivity was significantly enhanced at 0.15 bar. The spent activated carbons after vacuum regeneration exhibited stable CO_2 adsorption in five cycles, showing the high reusability for CO_2 capture.

Keywords Adsorption · Biomass · Carbon dioxide · Microporous materials · Pore volume

S. Deng (✉) · B. Hu · T. Chen · B. Wang · J. Huang · Y. Wang · G. Yu
School of Environment, Beijing Key Laboratory for Emerging Organic Contaminants Control, State Key Joint Laboratory of Environment Simulation and Pollution Control (SKLESPC), Tsinghua University, Beijing 100084, China
e-mail: dengshubo@tsinghua.edu.cn

1 Introduction

Carbon dioxide is a typical greenhouse gas responsible for anthropogenic global warming. The combustion of fossil fuel in power plants remains the main point source for CO_2 emission to the atmosphere. Among post-combustion CO_2 capture techniques, the amine-based chemical absorption system is considered as a suitable way (Rao and Rubin 2002), but the serious drawbacks such as volatility of the amines, facility corrosion and high energy consumption for regeneration, prevent its wide application. Alternatively, solid-based adsorbents have been drawn considerable attention for CO_2 capture in recent years (Choi et al. 2009; Wang et al. 2010; Hao et al. 2011).

Solid-based adsorbents for CO_2 adsorption mainly include zeolite (Zhang et al. 2010; Pham et al. 2013; Li and Tezel 2007), metal organic frameworks (Wu et al. 2010; Bae et al. 2009), activated carbon (Hu et al. 2011; Sethia and Sayari 2014; Nandi et al. 2012; Chen et al. 2013a; Rutherford and Coons 2003), nitrogen doped carbons (Gutierrez et al. 2011), metal oxide (Lee et al. 2008), and amine-modified porous materials (Chen et al. 2013b; Sakwa-Novak and Jones 2014; Khatri et al. 2006). Among these adsorbents, activated carbon has drawn great attention recently because of its high adsorption capacity, reversibility, stability and low cost (Choi et al. 2009). The adsorption performance of activated carbons is dependent on the selection of carbon sources and activation conditions. It has been reported that the activated carbons prepared with petroleum coke, sawdust, bamboo, celtuce leaves, polypyrrole and polyacrylonitrile fiber have high adsorption capacity for CO_2 (Hu et al. 2011; Nandi et al. 2012; Sevilla and Fuertes 2011; Wei et al. 2012; Wang et al. 2012; Saleh et al. 2013). Among different carbon sources, biomass is attractive due to its cost-effectiveness

and sustainability. KOH activation has been widely applied in the preparation of activated carbons because it can produce lots of micropores favorable for CO_2 adsorption (Hu et al. 2011), and the KOH/C mass ratios in the activation process are usually required to be high up to 2–4 (Hu et al. 2011; Sevilla and Fuertes 2011; Wei et al. 2012; Wang et al. 2012; Saleh et al. 2013). Since the textural properties of activated carbons and required KOH amount are closely related with the carbon precursors, it may be possible to find other biomass as carbon sources for the preparation of effective activated carbons at low KOH/C mass ratios.

In this study, we prepared the peanut shell and sunflower seed shell derived activated carbons at low KOH/C ratios, and the two activated carbons exhibited high adsorption capacity for CO_2 at 298 K and 0.15 bar. These biomass wastes have not been previously used as precursors to prepare activated carbons for CO_2 adsorption. The activation conditions including activation temperature and KOH/C mass ratio were optimized in the preparation. The activated carbons were characterized in terms of surface area, total pore volume, pore size distribution and surface morphology. To evaluate the activated carbons for CO_2 adsorption, the adsorption isotherm, selectivity, reusability and isosteric heat were measured and calculated. The relationship between the volume of micropore in the specific ranges and adsorbed amounts of CO_2 at 298 K and 0.15 bar was investigated, and the accurate micropore size range for CO_2 adsorption was proposed.

2 Experimental

2.1 Materials

The peanut shell and sunflower seed shell used in this study were collected by peeling the peanut and sunflower seeds purchased from a local market in Beijing. They were crushed and sieved in the size range of 10–30 mesh (2.0–0.59 mm). KOH was purchased from Beijing Modern Eastern Fine Chemical Company.

2.2 Preparation of biomass-derived activated carbons

The preparation of activated carbons consisted of carbonization and activation processes. The precursors including peanut shell and sunflower seed shell were first carbonized in a vacuum tubular furnace at 773 K for 1.5 h, and then the carbonized materials were impregnated with KOH solution at the predetermined KOH/C mass ratios for 48 h. The mixtures were dried at 378 K for 3 h and then heated in the vacuum tubular furnace again. The dried solids were first heated to 773 K at a ramping rate of 10 K/min, followed by heating to the predetermined activation temperature at a ramping rate of 5 K/min. After this temperature was kept for 1.5 h, the solids were cooled down to the ambient temperature. All the heating processes were conducted under N_2 flow protection (flow rate = 120 mL/min). The obtained solids were washed repeatedly with dilute HCl solution (1 mol/L) and deionized water until the pH value of washing water was less than 8.0. The activated carbons were finally obtained after drying at 378 K for 12 h. The peanut shell-derived activated carbon and sunflower seed shell-derived activated carbon are denoted as P-X-Y and S-X-Y, respectively, where X represents the activation temperature (K), and Y stands for the KOH/C mass ratio.

2.3 Characterization

Surface morphologies of the sunflower seed shell and sunflower seed as well as the activated carbons were characterized by a scanning electron microscopy (SEM, LEO-1530, LEO, Germany). The chemical composition of the samples was analyzed by an elemental analyzer (CE440, Exeter Analytical Inc., USA). The textural characteristics of the samples were measured by physical adsorption of N_2 at 77 K and CO_2 at 273 K using a gas adsorption instrument (Autosorb iQ, Quantachrome Corp., USA). The samples were outgassed at 300 °C for 4 h under vacuum condition. The specific surface area (S_{BET}) was calculated from the N_2 adsorption data using the Brunauer–Emmett–Teller (BET) equation in the relative pressure (P/P_0) range of 0.01–0.1, and the total pore volume (V_{total}) was calculated from the amount of N_2 adsorbed at $P/P_0 = 0.99$. An nonlocal density functional theory (NLDFT) model for CO_2 adsorption at 273 K was applied to determine the pore size (<1 nm) distribution and the cumulative pore volume.

2.4 CO_2 adsorption experiments

All CO_2 adsorption experiments were measured using a gas adsorption instrument (Autosorb iQ, Quantachrome Corp., USA). In the preparation optimization of activated carbons, CO_2 adsorption was carried out at 298 K, and the adsorbed amounts at 0.15 bar were compared. CO_2 adsorption isotherms were studied at 273 and 298 K, and the adsorption selectivity of CO_2 over N_2 on the activated carbons was evaluated by calculating their ratios of adsorbed amounts at 0.15 bar and 1 bar, which was denoted as $S(CO_2/N_2)$. The cyclic CO_2 adsorption- desorption was carried out for five times to study the reusability of the samples at 298 K. The regeneration of the samples was performed at 298 K under vacuum condition (<0.1 bar). The isosteric heat values were calculated from the CO_2 adsorption isotherms at 273 and 298 K by applying the Clausius-Clapeyron equation.

3 Results and discussion

3.1 Influence of activation condition on CO_2 adsorption

Activation conditions including KOH/C mass ratio and activation temperature significantly influence CO_2 adsorption. These two parameters were optimized to prepare the biomass-derived activated carbons with high CO_2 adsorption capacity at 298 K and 0.15 bar. When the KOH/C mass ratio was optimized, the activation temperature was fixed at 973 K. For the peanut shell, a series of samples were prepared at the KOH/C mass ratios ranging from 0.5 to 1.5. The adsorbed amounts of CO_2 first increased and then decreased with the increase of KOH/C mass ratios (Fig. 1a). An inflection point could be observed when the KOH/C mass ratio reached 1, and the highest CO_2 adsorbed amount was up to 1.54 mmol/g. As for the sunflower seed shell, the trend was the same as the peanut shell while the maximum CO_2 uptake of 1.46 mmol/g was obtained at the KOH/C mass ratio of 1.25 (Fig. 1a). Thus, the optimal KOH/C mass ratio was 1.0 for the peanut shell and 1.25 for the sunflower seed shell, which was adopted in the following experiments. The sharp decrease of CO_2 adsorption with further increasing KOH/C ratios indicated the collapse of the microporous structure under the over-intense activation conditions. It is noteworthy that even when the KOH/C ratio was as low as 0.50, the CO_2 uptake still reached 1.23 mmol/g (denoted as S-973-0.50).

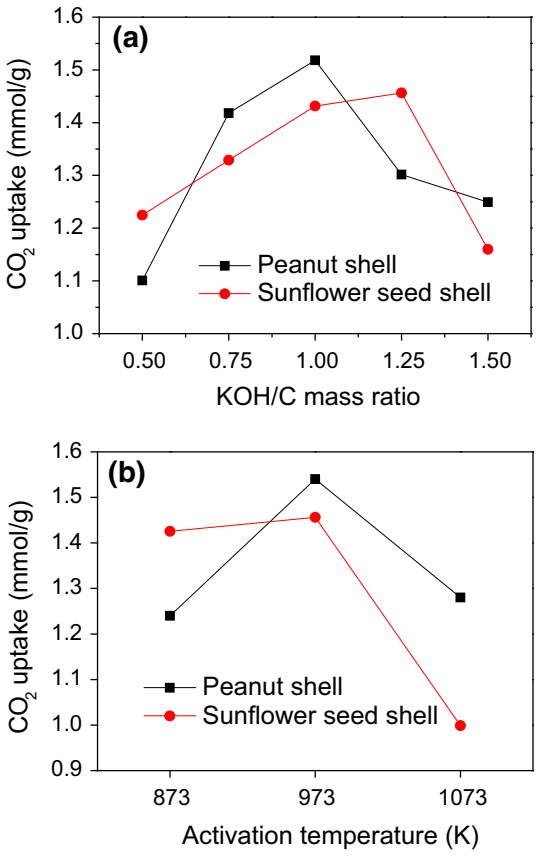

Fig. 1 Effect of KOH/C mass ratio (**a**) and activation temperature (**b**) on CO_2 adsorption at 298 K and 0.15 bar in the preparation of peanut shell and sunflower seed shell-derived activated carbons

After the KOH/C mass ratio was fixed, the activation temperature was changed from 873 K to 1,073 K. For the peanut shell, a peak value of CO_2 uptake was obtained at 973 K (Fig. 1b), and the as-prepared activated carbon was denoted as P-973-1.00. The sunflower seed shell had the same optimal activation temperature as the peanut shell, and the obtained activated carbon was denoted as S-973-1.25 (Fig. 1b). Therefore, both KOH/C mass ratio and activation temperature had significant influence on the preparation of biomass-derived activated carbons. The samples of P-973-1.00 and S-973-1.25 had CO_2 adsorption up to 1.54 and 1.46 mmol/g, respectively.

3.2 Adsorbent characterization

The elemental compositions of the activated carbons are shown in Table 1. The P-973-1.00 and S-973-1.25 have similar C content, but the P-973-1.00 has higher N content and lower O content than the S-973-1.25. The S-973-1.25 has the specific surface area of 1,790 m^2/g and total pore volume of 0.77 cm^3/g, much higher than the P-973-1.00.

According to the SEM images, the pristine sunflower seed shell has a unidirectional fibrous structure, and few pores are observed (Fig. 2a). After carbonization and activation, many micron-sized pores like pipes running through the carbons are observed, and there are some nanosized pores on the wall of "pipes" (Fig. 2b). In contrast, the pristine peanut shell also has the fibrous structure, and some micron-sized pores exist on the surface (Fig. 2d). After the activation, the parallel tubes are formed, and lots of nano-sized pores can be seen on the tube walls (Fig. 2d). Since the peanut shell derived activated carbon has higher wall thickness than sunflower seed shell derived one, it possesses higher mechanical strength. Lots of parallel tubes should facilitate the mass transfer of CO_2 molecules in the activated carbons, making CO_2 molecules easily diffuse into the micropores at low pressure than other activated carbons. The invisible nano-sized pores on the tube walls should be effective for CO_2 adsorption. These two activated carbons with this particular structure may be favorable for CO_2 adsorption at low pressure.

The narrow micropore size distribution (NMPSD) and cumulative pore volume (CPV) of P-973-1.00 and S-973-1.25 are shown in Fig. 3. Both activated carbons have three peaks in almost the same pore size ranges (Fig. 3a), and the pore volume of S-973-1.25 at the pore size of above 0.5 nm is larger than that of P-973-1.00, indicated a better developed microporous structure. Judging from the NMPSD and

Table 1 Physicochemical properties of the prepared biomass-derived activated carbon

Activated carbon	S_{BET} (m^2/g)	V_{total} (cm^3/g)	C (wt%)	H (wt%)	O (wt%)	N (wt%)
S-973-1.25	1,790	0.77	69.2	3.3	22.8	1.9
P-973-1.00	956	0.43	69.1	1.7	17.6	2.8

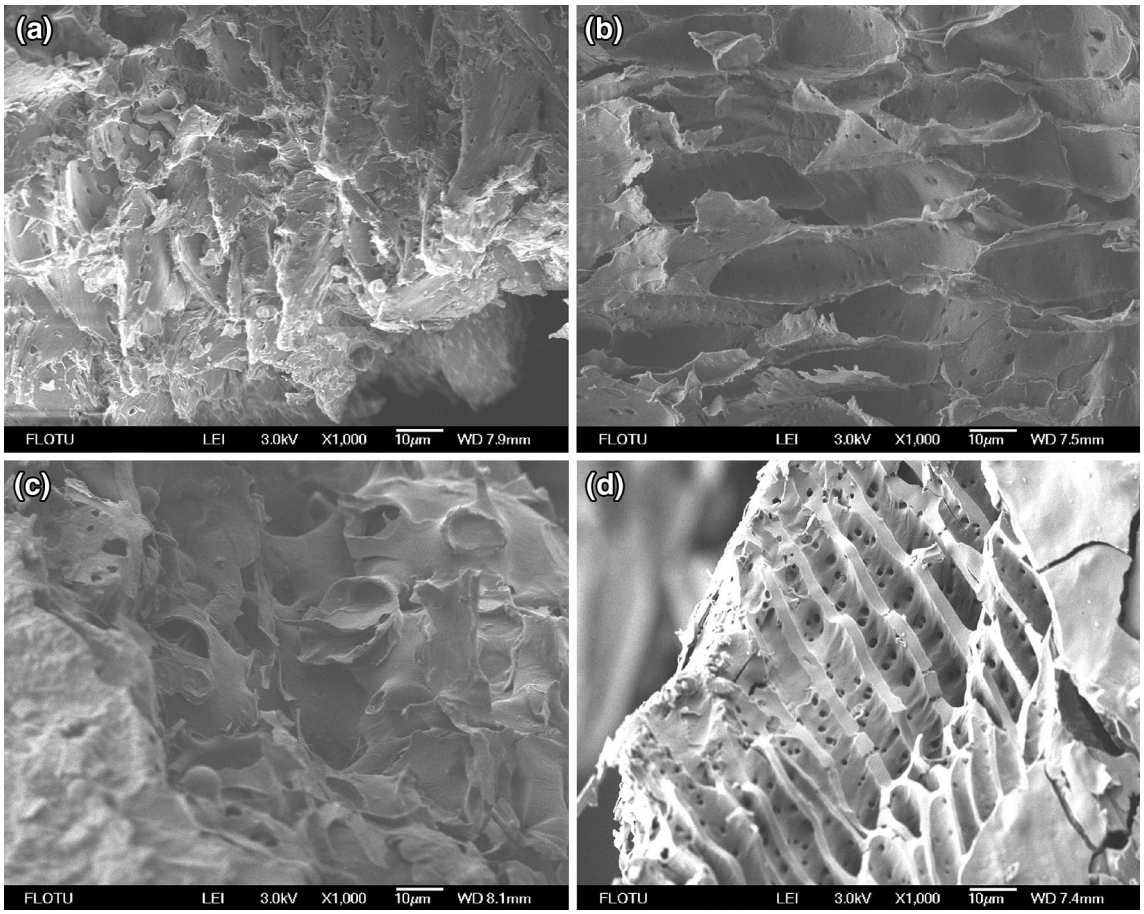

Fig. 2 SEM images of pristine sunflower seed shell (**a**), sunflower seed shell-derived activated carbon (**b**), pristine peanut shell (**c**), and peanut shell-derived activated carbon (**d**)

CPV, the P-973-1.00 has more micropores than S-973-1.25 until the pore size is less than 0.50 nm. The CPV of S-973-1.25 is about 50 % higher than that of P-973-1.00 when the pore diameter reaches 1.0 nm (Fig. 3b). Therefore, the S-973-1.25 has higher pore volume at the micropore size of less than 1 nm, but the P-973-1.00 possesses more narrow micropores in the range of 0.33–0.5 nm, which is favorable for CO_2 adsorption at high temperature and low pressure.

3.3 CO_2 adsorption capacity and selectivity

Figure 4 illustrates the adsorption isotherms of CO_2 at 273 and 298 K on the S-973-1.25 and P-973-1.00. It is interesting that the P-973-1.00 has higher CO_2 adsorption at 273 K than the S-973-1.25 at the pressure below 0.1 bar, while reverse trend is observed at the pressure above 0.1 bar. For CO_2 adsorption at 298 K, the P-973-1.00 exhibits higher adsorption capacity than the S-973-1.25 at the pressure below 0.3 bar. At 1 bar, the S-973-1.25 has high CO_2 uptake of 7.06 mmol/g at 273 K and 4.61 mmol/g at 298 K, much higher than 5.23 mmol/g at 273 K and 4.03 mmol/g at 298 K for P-973-1.00. With the decrease of CO_2 pressure, their difference in adsorption capacity becomes smaller, and even becomes reverse at low pressures. The adsorption capacity of CO_2 on both activated carbons decreases with increasing temperature since the

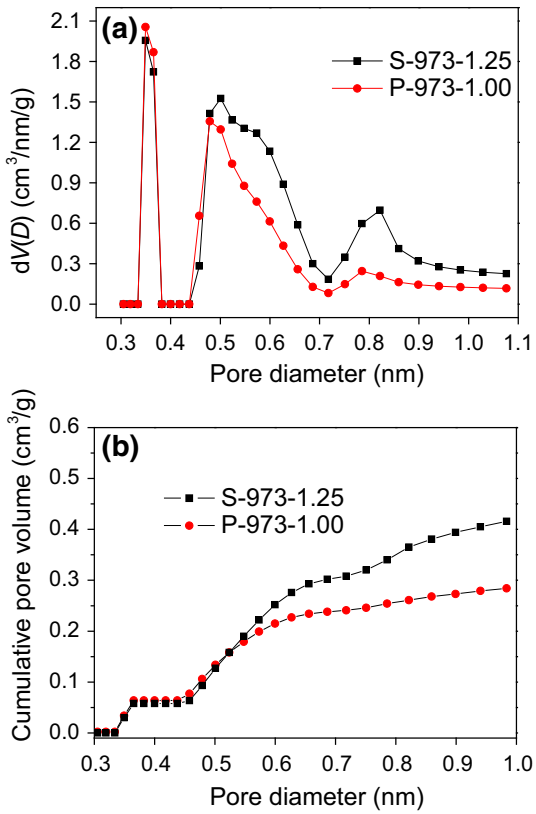

Fig. 3 Narrow micropore size distribution (**a**) and cumulative pore volume (**b**) of the S-973-1.25 and P-973-1.00

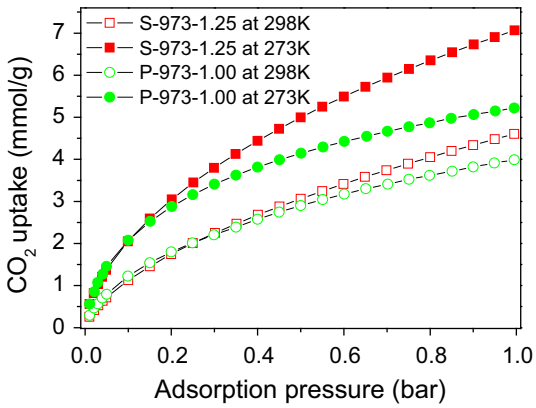

Fig. 4 Adsorption isotherms of CO_2 on the S-973-1.25 and P-973-1.00 at 273 K and 298 K

adsorption is an exothermic process. In comparison with P-973-1.00, the drop in CO_2 uptake on S-973-1.25 is more obvious when the temperature increases, especially when adsorption pressure is above 0.4 bar. This result is attributed to the more micropores in the range of 0.45–0.70 nm on the S-973-1.25, which contribute to CO_2 adsorption only at relatively high pressure. The P-973-1.00 has less micropores in this range, and thus the adsorption at relatively high pressure is low and insensitive to the change of temperature, resulting in the parallel isotherms after adsorption pressure above 0.4 bar. At 0.15 bar, the CO_2 uptake at 298 K on P-973-1.00 and S-973-1.25 was 1.54 mmol/g and 1.46 mmol/g, respectively (Fig. 4). The higher CO_2 adsorption on P-973-1.00 is closely related with its more micropores in the size range of 0.33–0.50 nm.

Since typical flue gas contains about 15 % CO_2 and 80 % N_2, the selective CO_2 adsorption over N_2 becomes an important criterion for the evaluation of activated carbons (Patino et al. 2012, 2014). Figure 5 shows the adsorption isotherms of CO_2 and N_2 at 298 K on S-973-1.25 and P-973-1.00. The S-973-1.25 exhibits a CO_2/N_2 selectivity [$S(CO_2/N_2)$ = adsorbed amount of CO_2 at 1 bar/adsorbed amount of N_2 at 1 bar] of 7.2 at 1 bar (Fig. 5a), and the P-973-1.25 has this selectivity of 5.6 (Fig. 5b). In consideration of CO_2 concentrations in flue gas, the selectivity based on the IAST method (Lee et al. 2013; Xie and Suh 2013) (selectivity = adsorbed amount of CO_2 at 0.15 bar/adsorbed amount of N_2 at 0.85 bar × 0.85/0.15) was calculated to be 14.9 for S-973-1.25 and 14.1 for P-973-1.00. Table 2 lists the adsorption capacity and selectivity of CO_2 on different activated carbons reported in the literature.

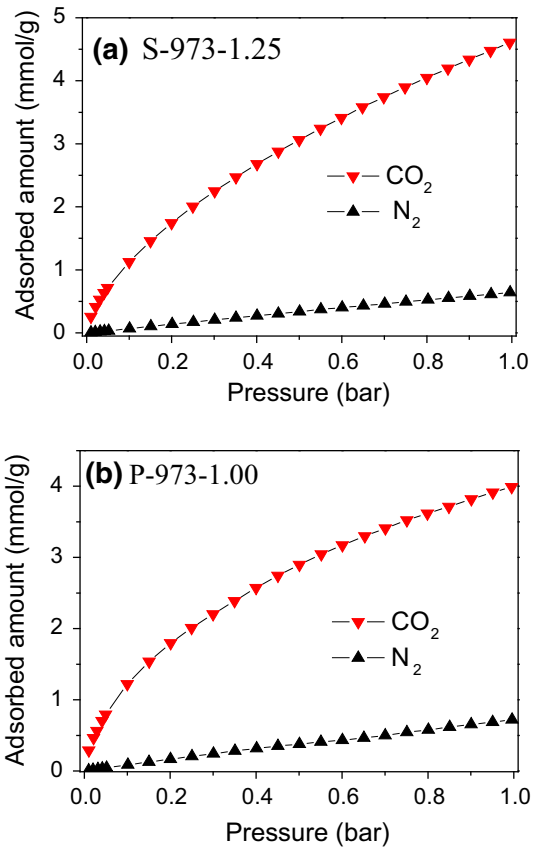

Fig. 5 Adsorption isotherms of CO_2 and N_2 on S-973-1.25 (**a**) and P-973-1.00 (**b**)

Table 2 Comparison of CO_2 adsorption at 298 K and 0.15 bar on activated carbons prepared from different precursors reported in the literature

Precursors	Activation agents	KOH/C mass ratio	S[CO_2/N_2] at 1 bar	CO_2 uptake (mmol/g)	Refs.
Petroleum pitch	KOH	3	2.8	1.1	Wahby et al. (2010)
Polyaniline	KOH	2	~11	1.7	Lin et al. (2014)
Polypyrrole	KOH	4	–	1.45	Meng and Park (2014)
Sawdust	KOH	2	5.4	1.2	Sevilla and Fuertes 2011
Bamboo	KOH	3	8.6	1.4	Wei et al. (2012)
Celtuce leaves	KOH	4	9.4	1.0	Wang et al. (2012)
Polyindole	KOH	52.3	~8	~1.6	Saleh et al. (2013)
Polyfurfuryl alcohol	KOH	2	6.5	~1	Sevilla and Fuertes 2012
Polyacrylonitrile fiber	Ar/CO_2	N/A	N/A	~1.3	Nandi et al. (2012)
Reduced-graphene-oxide/poly-thiophene	KOH	26.1	~21	~1.4	Seema et al. 2014
Phenylenediamine and terephthalaldehyde	KOH	2	5	~0.5	Wang et al. (2013)
Sunflower seed shell	KOH	1.25	7.2	1.46	This study
Peanut shell	KOH	1	5.6	1.54	This study

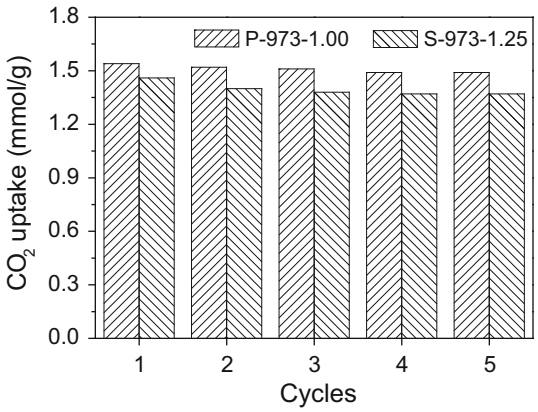

Fig. 6 CO_2 adsorption on the S-973-1.25 and P-973-1.00 at 298 K and 0.15 bar in the five cycles after vacuum regeneration

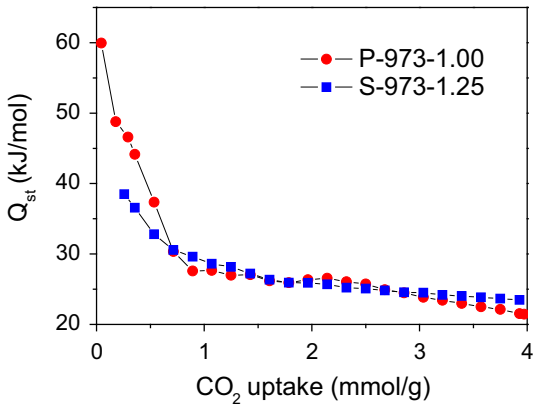

Fig. 7 Isosteric heat of CO_2 adsorption on the S-973-1.25 and P-973-1.00 calculated from adsorption isotherms at 273 and 298 K

Among these activated carbons, the sunflower seed shell-derived and peanut shell-derived activated carbons are among the adsorbents with the highest adsorption capacity for CO_2 and have moderate CO_2 selectivity over N_2. The higher CO_2 adsorption is attributed to the more micropores in the specific range mentioned above, while the moderate selectivity may be due to the narrow micropores, and the low content of nitrogen-containing groups on the adsorbents should have little contribution to CO_2 selectivity. The polyindole-derived carbon had high CO_2 adsorption of about 1.6 mmol/g, but this adsorbent was prepared at the superhigh KOH/C mass ratio of 52.3 (Saleh et al. 2013). The porous carbon prepared from polyaniline exhibits the highest adsorption capacity of about 1.7 mmol/g for CO_2 at 298 °C and 0.15 bar (Lin et al. 2014).

The spent activated carbons after CO_2 adsorption were regenerated via vacuum treatment at ambient temperature and reused to adsorb CO_2. Figure 6 presents the adsorbed amounts of CO_2 on the S-973-1.25 and P-973-1.00 in five consecutive adsorption–desorption cycles. The adsorbed amounts of CO_2 on the two samples all decreased slightly within the five cycles, and approached the stable values in the fifth cycle. The CO_2 uptake on P-973-1.00 and S-973-1.25 in the fifth cycle decreased by 6.2 and 3.2 %, respectively. The two activated carbons can be successfully regenerated by vacuum treatment and have promising application for CO_2 capture from actual flue gas.

According to the adsorption isotherms of CO_2 at 273 K and 298 K on the two activated carbons, the isosteric heat (Q_{st}) values of CO_2 adsorption were calculated and shown in Fig. 7. The Q_{st} values on P-973-1.00 are in the range of 21.5–60.0 kJ/mol for CO_2 uptake of 0.1–4.0 mmol/g, while the Q_{st} values on S-973-1.25 decrease from 38.5 to 23.5 kJ/mol when CO_2 uptake increases from 0.2 to 4.0 mmol/g. The higher Q_{st} values at lower CO_2 loading indicates the strong affinity of CO_2 to the adsorbents, which may be

related with the micropores in the activated carbons. Although the Q_{st} values are high, they are still much lower than the covalent bond energy, and thus the desorption process was reversible. By contrast, the Q_{st} values of both activated carbons in this study are higher than the activated carbon-based material (10.5–28.4 kJ/mol) (Guo et al. 2006) and the grapheme oxide based carbons (17–22 kJ/mol) (Srinivas et al. 2012). The Q_{st} values of P-973-1.00 are higher than these of the polyindole-derived activated carbon PIF6 (42.7 kJ/mol) (Saleh et al. 2013) and only a little lower than the activated carbon ACM-5 (65.2 kJ/mol) (Nandi et al. 2012).

3.4 Influence of textural properties of activated carbons on CO_2 adsorption

Several studies have revealed the relationship between micropore volume (MPV) and CO_2 adsorption (Hu et al. 2011; Sevilla and Fuertes 2011; Deng et al. 2014; Torregrossa-Macia et al. 1995). Wei et al. (2012) reported the relationship between the MPV of bamboo-derived activated carbon and CO_2 uptake at 273 K and 1 bar. It has been reported that the micropores smaller than 0.8 nm are effective for CO_2 adsorption at 273 K and 1 bar (Sethia and Sayari 2014), and the ranges of micropores responsible for CO_2 adsorption at different pressures at 273 K have also been studied (Primo et al. 2012). A series of sunflower seed shell-derived activated carbons were prepared, and their micropore volume in specific ranges and CO_2 uptake were correlated (Fig. 8). Because the kinetic diameter of CO_2 is 0.33 nm, the lower limit of the micropore size is fixed at 0.33 nm. Linear fitting was carried out on the plots of MPV at specific size range and CO_2 uptake, and the linear correlation coefficients (R^2) were obtained. When the upper limit of micropore sizes increases from 0.42 to 0.48 nm, R^2 first increases and then decreases, and the maximum R^2 (0.99) is obtained in the micropore range of 0.33–0.44 nm (Fig. 8b), indicating that CO_2 adsorption at 0.15 bar and 298 K is closely related with the volume of micropores in the range of 0.33–0.44 nm. Although the total pore volume of S-973-1.25 is higher than that of P-973-1.00 in the mocropore range of 0.33–1.0 nm, the P-973-1.00 has higher CO_2 adsorption at 0.15 bar and 298 K than S-973-1.25 due to the more micropores in the range of 0.33–0.44 nm for P-973-1.00. As shown in Table 2, different activated carbons exhibit different CO_2 uptake at 298 K and 0.15 bar, which is closely related with the pore volume ranging from 0.33 to 0.44 nm. Since the peanut shell and sunflower seed shell derived activated carbons in our study possess higher pore volume in the range of 0.33–0.44 nm, they exhibit higher CO_2 adsorption at 298 K and 0.15 bar. Nandi et al. (2012) reported that the activated carbon (ACM-5) had super high CO_2 uptake of 5.14 mmol/g at 298 K and 1 bar due to its rich

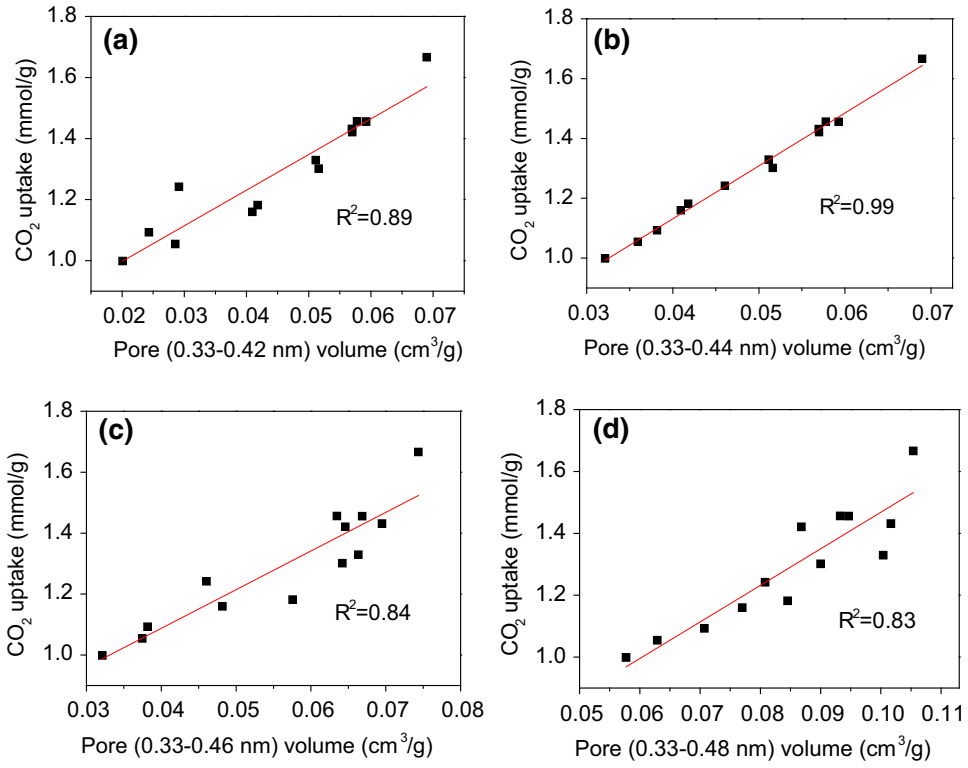

Fig. 8 Relationship between CO_2 adsorption and the micropore volume of sunflower seed shell-derived activated carbons in the range of **a** 0.33–0.42 nm, **b** 0.33–0.44 nm, **c** 0.33–0.46 nm, and **d** 0.33–0.48 nm

microporous structure, but most of these narrow micropores are around 0.7 nm in diameter, resulting in lower CO_2 adsorption at 298 K and 0.15 bar than the peanut shell and sunflower seed shell derived activated carbons. The micropore volume in the range of 0.33–0.82 nm was reported to have good linear relationship with the CO_2 uptake at 273 K and 1 bar (Wei et al. 2012). The range of micropores effective for CO_2 adsorption would narrow when the adsorption temperature increases and CO_2 pressure decreases.

4 Conclusions

The peanut shell and sunflower seed shell were used as cost-effective precursors to successfully prepare the activated carbons with high CO_2 adsorption. Such loose biomass is easy to form micropores at the low KOH/C ratios in the activation process. The cheap biomass cost and low KOH/C ratio make these two activated carbons more cost-effective than the conventional activated carbons. The two biomass-derived activated carbons exhibit higher CO_2 adsorption at 298 K and 0.15 bar than most of other activated carbons reported. The volume of micropores in the range of 0.33–0.44 nm has a linear relationship with the adsorbed amounts of CO_2 at 298 K and 0.15 bar, indicating that these micropores are responsible for CO_2 adsorption. The cost-effective peanut shell and sunflower seed shell derived activated carbons exhibit high adsorption capacity and moderate selectivity for CO_2 at low pressure as well as stable reusability, making them promising application in CO_2 capture from flue gas or air.

Acknowledgments We thank the Collaborative Innovation Center for Regional Environmental Quality, and Tsinghua University-Veolia Environnement Joint Research Center for Advanced Technology for financial support. Additionally, the analytical work was supported by the Laboratory Fund of Tsinghua University.

References

Bae, Y., Farha, O.K., Hupp, J.T., Snurr, R.Q.: Enhancement of CO_2/N_2 selectivity in a metal-organic framework by cavity modification. J. Mater. Chem. **19**, 2131–2134 (2009)

Chen, Z.H., Deng, S.B., Wei, H.R., Wang, B., Huang, J., Yu, G.: Activated carbons and amine-modified materials for carbon dioxide capture—a review. Front. Environ. Sci. Eng. **7**, 326–340 (2013a)

Chen, Z.H., Deng, S.B., Wei, H.R., Wang, B., Huang, J., Yu, G.: Polyethylenimine -impregnated resin for high CO_2 adsorption: an efficient adsorbent for CO_2 capture from simulated flue gas and ambient Air. ACS Appl. Mater. Interf. **5**, 6937–6945 (2013b)

Choi, S., Drese, J.H., Jones, C.W.: Adsorbent materials for carbon dioxide capture from large anthropogenic point sources. ChemSusChem **2**, 796–854 (2009)

Deng, S.B., Wei, H.R., Chen, Z.H., Wang, B., Huang, J., Yu, G.: Superior CO_2 adsorption on pine nut shell-derived activated carbons and the effective micropores at different temperatures. Chem. Eng. J. **253**, 46–54 (2014)

Guo, B., Chang, L., Xie, K.: Adsorption of carbon dioxide on activated carbon. J. Nat. Gas Chem. **15**, 223–229 (2006)

Gutierrez, M.C., Carriazo, D., Ania, C.O., Parra, J.B., Ferrera, M.L., del Monte, F.: Deep eutectic solvents as both precursors and structure directing agents in the synthesis of nitrogen doped hierarchical carbons highly suitable for CO_2 capture. Energy Environ. Sci. **4**, 3535–3544 (2011)

Hao, G., Li, W., Lu, A.: Novel porous solids for carbon dioxide capture. J. Mater. Chem. **21**, 6447–6451 (2011)

Hu, X., Radoszka, M., Cychosz, K.A., Thommes, M.: CO_2-filling capacity and selectivity of carbon nanopores: synthesis, texture, and pore-size distribution from quenched-solid density functional theory (QSDFT). Environ. Sci. Technol. **45**, 7068–7074 (2011)

Khatri, R.A., Chuang, S.S.C., Soong, Y., Gray, M.: Thermal and chemical stability of regenerable solid amine sorbent for CO_2 capture. Energy Fuel. **4**, 1514–1520 (2006)

Lee, D., Zhang, C.Y., Wei, C., Ashfeld, B.L., Gao, H.F.: Hierarchically porous materials via assembly of nitrogen-rich polymer nanoparticles for efficient and selective CO_2 capture. J. Mater. Chem. A **1**, 14862–14867 (2013)

Lee, S.C., Chae, H.J., Lee, S.J., Choi, B.Y., Yi, C.K., Lee, J.B., Ryu, C.K., Kim, J.C.: Development of regenerable MgO-based sorbent promoted with K_2CO_3 for CO_2 capture at low temperatures. Environ. Sci. Technol. **42**, 2736–2741 (2008)

Li, P.Y., Tezel, F.H.: Adsorption separation of N_2, O_2, CO_2 and CH_4 gases by β-zeolite. Micropor. Mesopor. Mater. **98**, 94–101 (2007)

Lin, D.H., Zhang, X.T., Cui, X.W., Chen, W.X.: Highly porous carbons with superior performance for CO_2 capture through hydrogen-bonding interactions. RSC Adv. **4**, 27414–27421 (2014)

Meng, L.Y., Park, S.J.: One-pot synthetic method to prepare highly N-doped nanoporous carbons for CO_2 adsorption. Mater. Chem. Phys. **143**, 1158–1163 (2014)

Nandi, M., Okada, K., Dutta, A., Bhaumik, A., Maruyama, J., Derks, D., Uyama, H.: Unprecedented CO_2 uptake over highly porous N-doped activated carbon monoliths prepared by physical activation. Chem. Commun. **48**, 10283–10285 (2012)

Patino, J., Gutierrez, M.C., Carriazo, D., Ania, C.O., Parra, J.B., Ferrer, M.L., del Monte, F.: Deep eutectic assisted synthesis of carbon adsorbents highly suitable for low-pressure separation of CO_2-CH4 gas mixtures. Energy Environ. Sci. **5**, 8699–8707 (2012)

Patino, J., Gutierrez, M.C., Carriazo, D., Ania, C.O., Fierro, J.L.G., Ferrera, M.L., del Monte, F.: DES assisted synthesis of hierarchical nitrogendoped carbon molecular sieves for selective CO_2 versus N_2 adsorption. J. Mater. Chem. A **2**, 8719–8729 (2014)

Pham, T.D., Liu, Q., Lobo, R.F.: Carbon dioxide and nitrogen adsorption on cation-exchanged SSZ-13 zeolites. Langmuir **29**, 832–839 (2013)

Primo, A., Forneli, A., Corma, A., Garcia, H.: From biomass wastes to highly efficient CO_2 adsorbents: graphitisation of chitosan and alginate biopolymers. ChemSusChem **5**, 2207–2214 (2012)

Rao, A.B., Rubin, E.S.: A technical, economic, and environmental assessment of amine-based CO_2 capture technology for power plant greenhouse gas control. Environ. Sci. Technol. **36**, 4467–4475 (2002)

Rutherford, S.W., Coons, J.E.: Adsorption dynamics of carbon dioxide in molecular sieving carbon. Carbon **41**, 405–411 (2003)

Sakwa-Novak, M.A., Jones, C.W.: Steam induced structural changes of a poly(ethylenimine) impregnated gamma-alumina sorbent for CO_2 extraction from ambient air. ACS Appl. Mater. Interf. **6**, 9245–9255 (2014)

Saleh, M., Tiwari, J.N., Kemp, K.C., Yousuf, M., Kim, K.S.: Highly selective and stable carbon dioxide uptake in polyindole-derived microporous carbon materials. Environ. Sci. Technol. **47**, 5467–5473 (2013)

Seema, H., Kemp, K.C., Le, N.H., Park, S., Chandra, V., Lee, J.W., Kim, K.S.: Highly selective CO_2 capture by S-doped microporous carbon materials. Carbon **66**, 320–326 (2014)

Sethia, G., Sayari, A.: Nitrogen-doped carbons: remarkably stable materials for CO_2 capture. Energy Fuel. **28**, 2727–2731 (2014)

Sevilla, M., Fuertes, A.B.: Sustainable porous carbons with a superior performance for CO_2 capture. Energy Environ. Sci. **4**, 1765–1771 (2011)

Sevilla, M., Fuertes, A.B.: CO_2 adsorption by activated templated carbons. J. Colloid Interf. Sci. **366**, 147–154 (2012)

Srinivas, G., Burress, J., Yildirim, T.: Graphene oxide derived carbons (GODCs): synthesis and gas adsorption properties. Energy Environ. Sci. **5**, 6453–6459 (2012)

Torregrossa-Macia, R., Martin-Martinez, J.M., Mittelmeijer-Hazeleger, M.C.: Mechanisms of adsorption of CO_2 in the micropores of activated anthracite. Fuel **74**, 111–114 (1995)

Wahby, A., Ramos-Fernández, J.M., Martínez-Escandell, M., Sepúlveda-Escribano, A., Silvestre-Albero, J., Rodríguez-Reinoso, F.: High-surface-area carbon molecular sieves for selective CO_2 adsorption. ChemSusChem **3**, 974–981 (2010)

Wang, J., Senkovska, I., Oschatz, M., Lohe, M.R., Borchardt, L., Heerwig, A., Liu, Q., Kaskel, S.: Highly porous nitrogen-doped polyimine-based carbons with adjustable microstructures for CO_2 capture. J. Mater. Chem. A **1**, 10951–10961 (2013)

Wang, Q., Luo, J., Zhong, Z., Borgna, A.: CO_2 capture by solid adsorbents and their applications: current status and new trends. Energy Environ. Sci. **4**, 42–55 (2010)

Wang, R., Wang, P., Yan, X., Lang, J., Peng, C., Xue, Q.: Promising porous carbon derived from celtuce leaves with outstanding supercapacitance and CO_2 capture performance. ACS Appl. Mater. Interf. **4**, 5800–5806 (2012)

Wei, H.R., Deng, S.B., Hu, B., Chen, Z., Wang, B., Huang, J., Yu, G.: Granular bamboo-derived activated carbon for high CO_2 adsorption: The dominant role of narrow micropores. ChemSusChem **5**, 2354–2360 (2012)

Wu, D., Xu, Q., Liu, D., Zhong, C.: Exceptional CO_2 capture capability and molecular-level segregation in a Li-modified metal–organic framework. J. Phys. Chem. C **114**, 16611–16617 (2010)

Xie, L.H., Suh, M.P.: High CO_2-capture ability of a porous organic polymer bifunctionalized with carboxy and triazole groups. Chem. Eur. J. **19**, 11590–11597 (2013)

Zhang, Z., Zhang, W., Chen, X., Xia, Q., Li, Z.: Adsorption of CO_2 on zeolite 13X and activated carbon with higher surface area. Sep. Sci. Technol. **45**, 710–719 (2010)